Universiteit
Leiden
The Netherlands

PIN protein phosphorylation by plant AGC3 kinases and its role in polar auxin transport

Huang, F.

Citation
Huang, F. (2010, September 1). *PIN protein phosphorylation by plant AGC3 kinases and its role in polar auxin transport*. Retrieved from https://hdl.handle.net/1887/15916

Version:	Not Applicable (or Unknown)
License:	Leiden University Non-exclusive license
Downloaded from:	https://hdl.handle.net/1887/15916

Note: To cite this publication please use the final published version (if applicable).

Chapter 4

PINOID-mediated phosphorylation reduces vacuolar targeting of the PIN1 auxin efflux carrier by enhancing plasma membrane localization

Fang Huang, Jan Petrásek[1], Eva Zazimilova[1], Remko Offringa

[1] Institute of Experimental Botany, Academy of Sciences of the Czech Republic, 165 02 Prague 6, Czech Republic.

Abstract

The plant hormone auxin regulates a plethora of plant developmental programs through polar auxin transport (PAT) generated maxima and minima. Key drivers of this cell to cell transport are the PIN efflux carriers that determine the direction of auxin flow through their asymmetric distribution at the plasma membrane (PM). PIN abundance and polar localization are regulated by a dynamic process of endocytosis and recycling to the PM, or alternatively targeting to the vacuole for degradation. The PINOID (PID) serine/threonine protein kinase has been shown to direct apical PIN targeting by phosphorylating PIN proteins in their central hydrophilic loop (HL) at serine residues located in three conserved TPRXS(N/S) motifs. Here, we further investigated the role of PID phosphorylation in PAT, by affecting PIN1 intracellular trafficking. By inducible expression of PID in tobacco BY-2 cells, we confirm the role of PID as positive regulator of auxin efflux. Expression of wild type or non-phosphorylatable PIN1:GFP versions in *Arabidopsis* protoplasts showed that phosphorylation at the TPRXS(N/S) motifs reduced the rate of PIN1 targeting to the vacuoles. Also in seedling roots, non-phosphorylatable or phosphomimic PIN1:GFP proteins showed respectively enhanced or reduced vacuolar targeting compared to wild type PIN1:GFP. Collectively, our data indicate that besides the function as PIN polarity determinant, PID promotes auxin efflux by phosphorylating PIN1 at the TPRXS(N/S) motifs to enhance their PM localization, and as a result reduce PIN1 targeting to and degradation in the vacuole.

Introduction

Cellular signaling and transport processes are mediated by plasma membrane (PM) receptors or transporters whose abundance at the PM is regulated by targeting of newly synthesized proteins to the PM, subsequent endocytosis and recycling, or sending the internalized proteins to the vacuole for degradation. A well studied transport process in plants that is regulated by the PM abundance and subcellular distribution of the transporters is the polar cell to cell transport of the plant hormone auxin by the PIN efflux carriers. Auxin regulates basic cellular processes such as cell division, -growth and –differentiation, and affects almost every aspect of plant development through its polar transport-generated maxima and minima (Tanaka et al., 2006; Sorefan et al., 2009). In the model plant *Arabidopsis thaliana*, the PIN family is composed of eight members, of which the PIN1-type proteins (PIN1, PIN2, PIN3, PIN4 and PIN7) are now recognized as the drivers of polar auxin transport (PAT) that determine the direction of auxin flow through their asymmetric distribution at the PM (Petrásek et al., 2006; Wiśniewska et al., 2006;

Mravec et al., 2009). This asymmetric localization is dynamic and can be modulated by developmental signals (Benková et al., 2003; Friml et al., 2003b), environmental cues (Friml et al., 2002b; Harrison and Masson, 2008) and auxin levels (Paciorek et al., 2005; Sauer et al., 2006), through cellular trafficking mechanisms that have been extensively investigated.

PIN protein trafficking has been most extensively investigated for *Arabidopsis* PIN1 and PIN2, and these studies have led to the model that, following their synthesis PIN proteins are placed at the PM in an apolar manner, and that polarity is subsequently established and maintained by constitutive endocytosis and recycling of PIN cargoes between the PM and endosomes (Geldner et al., 2001; Dhonukshe et al., 2008). Recycling from the endosomes to the basal (rootward) PM is mediated by the ADP-ribosylation factor guanine nucleotide exchange factor (ARF-GEF) GNOM (Steinmann et al., 1999; Geldner et al., 2003), which is a target of the fungal toxin brefeldin A (BFA) (Geldner et al., 2003). Short-term BFA treatment induces reversible intracellular accumulation of PIN1 protein in BFA compartments (Geldner et al., 2001). In contrast, apical localized PINs are less sensitive to the GNOM inhibitor BFA, indicating that apical recycling is mediated by another BFA-insensitive ARF-GEF. In line with this conclusion, long-term BFA treatment induces transcytosis of basally localized PINs to the apical (shootward) domain (Kleine-Vehn et al., 2008a).

The same basal-to-apical polarity switch can also be achieved by the activity of the PINOID (PID) protein kinase. In root cells, a high dose of PID activity (*PID* overexpression) induces a basal-to-apical PIN polarity switch and a depletion of the organizing auxin maximum, subsequently leading to agravitropic root growth and collapse of the primary root meristem. In contrast, in the embryo and the inflorescence meristem, a low dose of PID (*pid* loss-of-function) causes an apical-to-basal PIN1 polarity shift, resulting in pin-like inflorescences and defects in auxin-related embryo development (Friml et al., 2004). Recently it was shown that PID phosphorylates PIN proteins in their central hydrophilic loop (HL), and that it acts antagonistically with PP2A phosphatases to induce PIN polarity change (Michniewicz et al., 2007). Further analysis showed that PID phosphorylation regulates PIN polarity by recruiting them from the basal recycling pathway to the GNOM-independent apical recycling pathway (Kleine-Vehn et al., 2009).

The abundance of PM PIN proteins, for example PIN2, was also shown to be regulated by its internalization and subsequent vacuolar targeting for degradation during root gravitropic response (Abas et al., 2006; Kleine-Vehn et al., 2008b; Laxmi et al., 2008). This process requires proteasome-dependent PIN ubiquitination, and was shown to be regulated by HY5-dependent light signaling, and to involve the COP9 signalosome and the 26S proteasome (Laxmi et al., 2008).

Previous studies suggested that the PID kinase, besides its role as a PIN polarity

determinant, is also a positive regulator of PAT (Benjamins et al., 2001; Lee and Cho, 2006). This implies that phosphorylation by PID is likely to affect PIN PM abundance. In Chapter 2, we showed that PID phosphorylates serine residues present in three conserved TPRXS(N/S) motifs in the PIN1HL. Here we used the mutant constructs and plant lines generated for these studies to show that in the dark loss-of-phosphorylation PIN1 proteins exhibit an enhanced relocation from PM to vacuoles both in *Arabidopsis* protoplasts, and in *Arabidopsis* embryos and seedling roots. This vacuolar targeting could be inhibited by light, by treatment with the 26S proteasome inhibitor MG132, or by co-expression of the PID kinase. Our results indicate that apart from PIN polarity establishment, PID also determines auxin transport by enhancing PM localization of PINs, and as a result reducing their vacuolar targeting.

Results and discussion

PID activity enhances auxin efflux in tobacco BY-2 cells

To find direct evidence for the positive effect of PID on auxin efflux, the *pINTAM>>PID* construct for tamoxifen inducible expression of PID was introduced via *Agrobacterium*-mediated transformation into tobacco BY-2 cells or into the transgenic BY-2 cell line expressing *PIN1::PIN1:GFP* (Zažímalová et al., 2007). Semi-quantitative RT-PCR analysis clearly showed that PID expression was nicely induced following tamoxifen treatment in both the *pINTAM>>PID* and the *pINTAM>>PID+PIN1::PIN1:GFP* transgenic cell lines (Figure 1A). PIN1:GFP was well expressed and localized at the PM in the *pINTAM>>PID+PIN1::PIN1:GFP* transgenic line (Figure 1B). This cell line was used to measure the retention of ^{3}H-NAA after 48 hours (hrs) treatment with 5 mM tamoxifen. Compared to the non-induced (DMSO treated) control cell line, ^{3}H-NAA retention was significantly reduced when PID expression was induced (Figure 1C). This result corroborated the previously suggested role for PID as positive regulator of auxin efflux (Benjamins et al., 2001; Lee and Cho, 2006), and indicated that PID-dependent phosphorylation of PIN proteins stimulates their PM localization, either by inhibiting endocytosis, or by enhancing exocytosis.

PIN1:GFP localizes at the PM and in endosomal structures, and accumulates in the vacuoles in *Arabidopsis* protoplasts

To further analyze the effect of phosphorylation on PIN subcellular trafficking, we firstly used transfection of *Arabidopsis* cell suspension-based protoplasts as an easy and efficient system to analyze the subcellular localization of PIN1 proteins. When protoplasts were transfected with *35S::PIN1:GFP*, PIN1:GFP was not only observed at

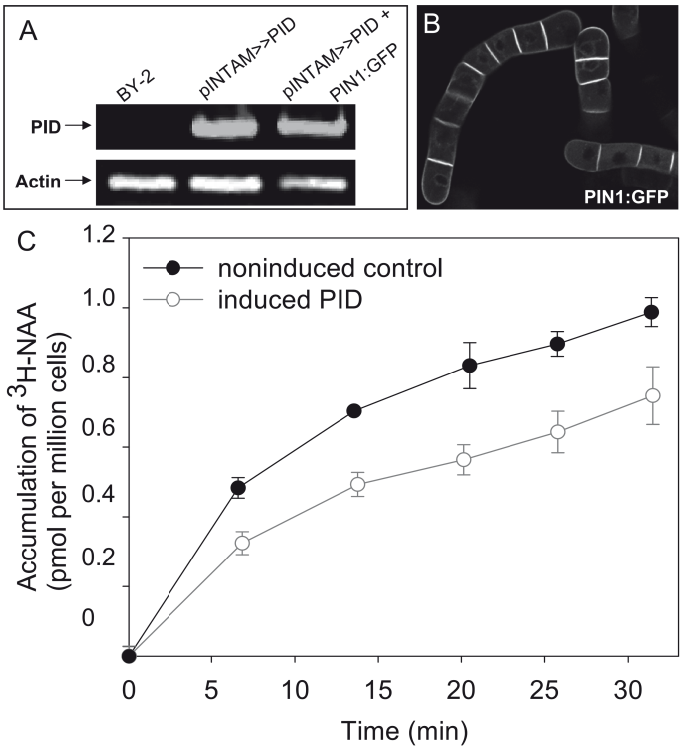

Figure 1. Inducible *PID* expression enhances auxin efflux from tobacco BY2 cells.
(A) Semi quantitative RT-PCR analysis detects *PID* expression in the transgenic *pINTAM>>PID* or *pINTAM>>PID* + *PIN1:GFP* BY-2 cells, but not in non transgenic BY-2 cells after 48 hrs induction with 5 uM tamoxifen
(B) PIN1:GFP localization in *pINTAM>>PID* + *PIN1:GFP* BY-2 cells
(C) Accumulation of ^{3}H-NAA (2 nM) in *pINTAM>>PID* + *PIN1:GFP* BY-2 cells after 48 hrs treatment with DMSO (non-induced control) or 5 uM tamoxifen (induced PID).

the PM and at intracellular punctuates (Figure 2A), consistent with previous observations (Dhonukshe et al., 2007), but also in vacuole-like structures (Figure 2B). Similarly, in the *pINTAM>>PID+PIN1::PIN1:GFP* BY-2 cell line (DMSO control), PIN1:GFP proteins were not only PM localized (Figure 2C), but also found accumulating in the vacuole-like structures (Figure 2D).

To characterize these GFP containing compartments, transfected *Arabidopsis* protoplast cells were treated with FM4-64, an endocytic marker that has been reported to fluorescently label the tonoplast within 2 hrs incubation (Dettmer et al., 2006). With time lapses, FM4-64 stain occurred gradually, first from the PM to endosomes, and finally reaching the tonoplast (Figure 2E). In the same cell, a diffused GFP signal was detected in the lumen of the vacuole surrounded by FM4-64 stain (Figure 2F and 2G),

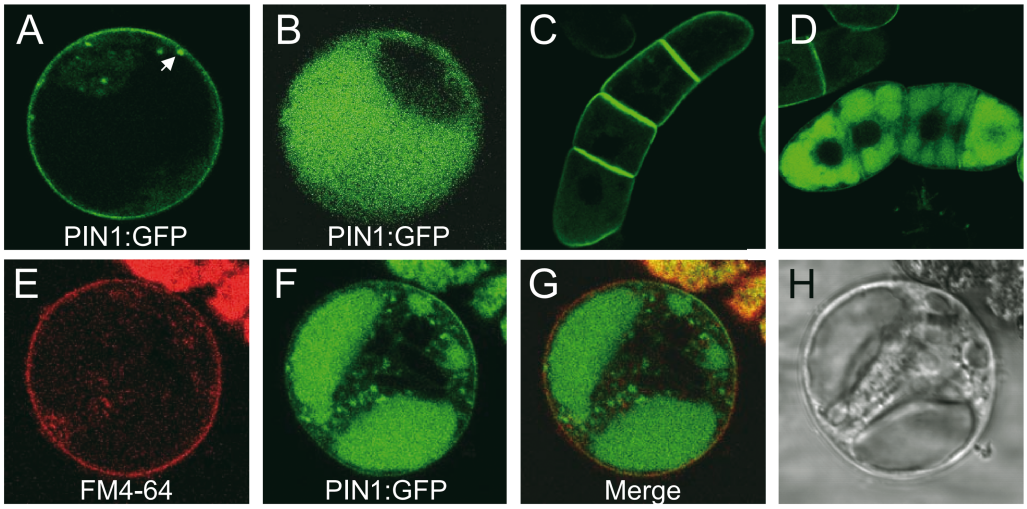

Figure 2. PIN1:GFP shows vacuolar accumulation in *Arabidopsis* protoplasts and tobacco BY-2 cells.
(A) PIN1:GFP transfected protoplasts show GFP signal at the PM and at endosomal punctuate structures (arrow).
(B) At increasing time point after transfection, more cells show PIN1:GFP signal in the vacuole-like structure.
(C) PIN1:GFP PM localization in tobacco BY-2 suspension cells
(D) PIN1:GFP accumulation in the vacuole-like structures in tobacco BY-2 suspension cells
(E) to **(H)** Characterization of GFP-accumulated vacuolar compartments
After pulse-labeling with FM4-64 for 1 hr, the fluorescent stain is internalized and starts to accumulate on the tonoplast **(E)**. In the same cell, PIN1:GFP was detected in the FM4-64 marked vacuole (**[F]** and **[G]**), which is also distinguishable in the bright field image **(H)**.

which was recognized in the bright field imaging as well (Figure 2H). Our data indicated that PIN1:GFP undergoes a dynamic re-location from the PM to endosomes, and finally to vacuolar compartments.

PID-dependent phosphorylation reduces PIN1 vacuolar targeting in a dose-dependent manner.

The dynamic PIN1 subcellular localization in *Arabidopsis* protoplast cells allowed us to investigate the effect of PID-phosphorylation on PIN1 intracellular trafficking. Previously, the serine residues located in three conserved TPRXS(N/S) motifs in PIN1HL were identified to be phosphorylation targets of PID (Huang et al., 2010). Various mutant constructs were generated from *35S::PIN1:GFP*, in which one, two, or all serines (S) in the encoded PIN1:GFP proteins were replaced by nonphosphorylatable alanines (A). The resulting constructs *35S::PIN1:GFP, 35S::PIN1:GFP S1A, 35S::PIN1:GFP S1,3A* and *35S::PIN1:GFP S1,2,3A* (hereafter referred to as *PIN1:GFP*, *PIN1:GFP S1A*,

PIN1:GFP S1,3A and *PIN1:GFP S1,2,3A*) were transfected into protoplasts alone, or co-transfected with *35S::PID:mRFP* (hereafter referred to as *PID:RFP*). The protoplasts were incubated in darkness for 17, 19, 21 and 23 hrs after transfection and fluorescent signals were observed by confocal laser scanning microscopy. The frequency of cells with vacuolar GFP signal was determined by dividing the number of cells with vacuolar GFP signal by the total number of PIN1:GFP expressing cells (n>80).

When transfected with *PIN1:GFP* alone, the frequency of protoplasts with vacuolar signal increased with time (Figure 3, black), indicating that PIN1:GFP first occurs at the PM and then gradually is targeted to the vacuole. Interestingly, the vacuolar GFP signal observed following *PIN1:GFP* transfection was greatly reduced (from 60% to 20% at 17 hrs) compared to the cells co-transfected with *PID:RFP* (Figure 3, black and dark gray), indicating that PID activity reduces PIN1 vacuolar targeting. In line with this, no significant difference in vacuolar accumulation was observed when *PIN1:GFP S1,2,3A* was transfected alone or in combination with *PID:RFP* (Figure 3, light gray and white), corroborating that PID-dependent phosphorylation at the TPRXS(N/S) motifs reduces vacuolar targeting of PIN1:GFP. Moreover, *PIN1:GFP S1,2,3A* vacuolar accumulation was slightly enhanced compared to *PIN1:GFP* transfection (from 62% to 75% at 19 hrs) (Figure 3, black and light gray), suggesting that the endogenous kinase activity in protoplasts is sufficient to distinguish phosphorylatable PIN1 substrates from non-phosphorylatable ones.

Compared to the *PIN1:GFP* transfection, cotransfection of the mutant constructs

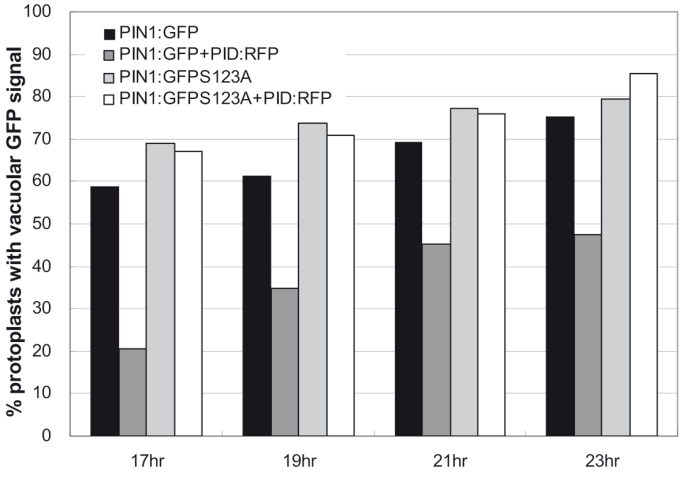

Figure 3. PID-mediated phosphorylation reduces PIN1:GFP vacuolar targeting in *Arabidopsis* protoplasts. *Arabidopsis* protoplasts were transfected with *PIN1:GFP* (black) or *PIN1:GFP S1,2,3A* (light gray), co-tranfected with *PIN1:GFP* and *PID:RFP* (dark gray), or *PIN1:GFP S1,2,3A* and *PID:RFP* (white). Protoplasts were observed and counted after incubation in darkness for 17 hrs up to 23 hrs.

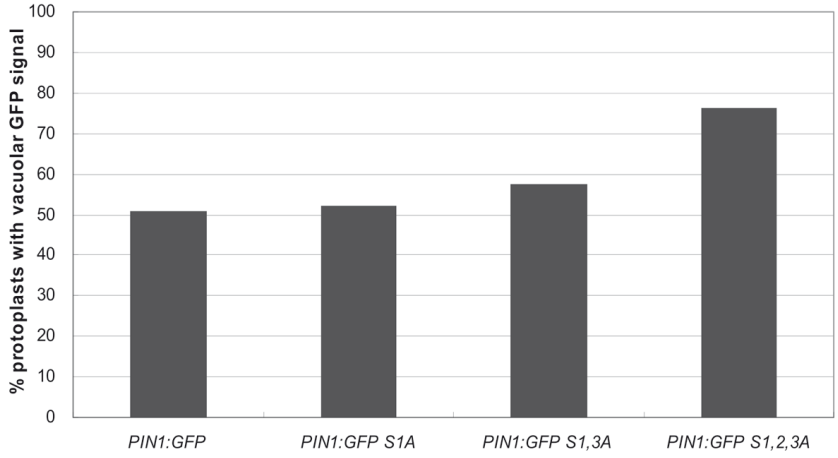

Figure 4. Reduction in PIN1:GFP vacuolar targeting is phosphorylation dose-dependent.
Arabidopsis protoplasts were co-transfected with *PID:RFP* and *PIN1:GFP*, *PIN1:GFP S1A*, *PIN1:GFP S1,3A* or *PIN1:GFP S1,2,3A*, and were observed and counted after incubation in darkness for 19 hrs.

PIN1:GFP S1A, PIN1:GFP S1,3A, or *PIN1:GFP S1,2,3A* with *PID:RFP* increased the frequency of protoplasts with the vacuolar GFP signal from 50% to respectively, 52%, 57% and 76% at 19 hrs (Figure 4). The additive effect of one, two or three non-phosphorylatable serines on enhancing PIN1 vacuolar targeting indicates that the effect of phosphorylation on PIN1 subcellular trafficking is dose dependent.

Light and phosphorylation control PIN1 vacuolar accumulation at different check points.

It has been shown that PIN1 exhibits vacuolar accumulation in dark-grown seedling roots (Laxmi et al., 2008) and leaf primordia (Shirakawa et al., 2009). In our studies, transfected protoplasts were standardly incubated in darkness. In order to test if the vacuolar accumulation of GFP observed in our analysis could be influenced by light treatment, protoplasts co-transfected with *PIN1:GFP* (or *PIN1:GFPS1,2,3A*) and *PID:RFP*, following an initial 17 hrs dark incubation, were incubated in light or dark for different time periods. Light treatment reduced vacuolar GFP accumulation for both co-transfections, and this reduction became more significant after longer incubation (Figure 5), indicating that in *Arabidopsis* protoplasts PIN1 vacuolar targeting is negatively regulated by light, consistent with what has previously been reported (Laxmi et al., 2008). At the start of the light treatment, 20% of the *PIN1:GFP* transfected protoplasts and 70% of the *PIN1:GFP S1,2,3A* transfected protoplasts showed vacuolar GFP signal, and 6 hrs light treatment reduced this percentage to respectively 10% and 40%, around half of the starting level (Figure 5). This observation suggested that light might regulate PIN1 vacuolar targeting

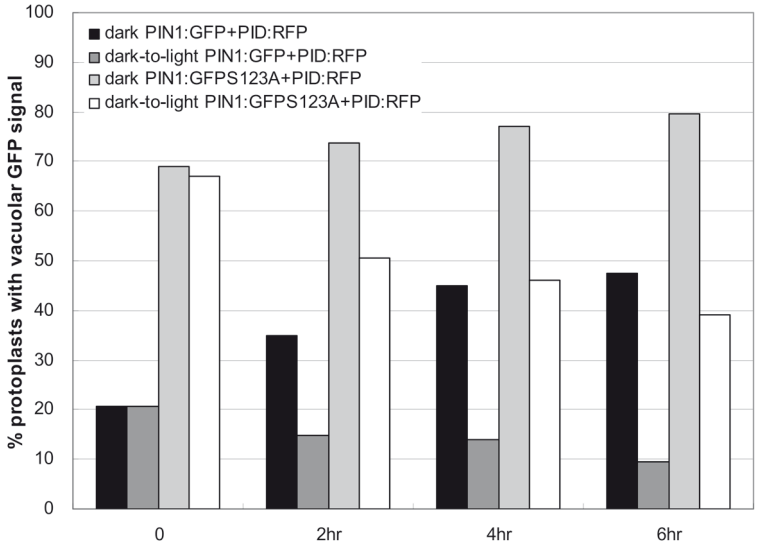

Figure 5. PID-mediated phosphorylation and light reduce PIN1:GFP vacuolar targeting via independent pathways.

Arabidopsis protoplasts co-transfected with *PIN1:GFP* and *PID:RFP* (black and dark gray) or *PIN1:GFP S1,2,3A* and *PID:RFP* (light gray and white) were first incubated in continuous darkness for 17 hrs and then observed and counted after 2, 4 and 6 hrs in the dark (black and light gray) or in the light (dark gray and white).

downstream of phosphorylation regulation at different check point. Together, these results confirm our earlier conclusion that PID-dependent phosphorylation negatively regulates PIN1 vacuolar targeting, and the combined effects of light and phosphorylation on PIN1 vacuolar targeting suggest that these inputs function at different check points in the process.

Phosphorylation reduces PIN1:GFP vacuolar targeting and degradation *in planta*. To confirm our in protoplast observations in *planta*, we used previously generated transgenic lines expressing *PIN1::PIN1:GFP* or *PIN1::PIN1:GFP S1,2,3A(E)* constructs in the *pin1* mutant background (referred to as *PIN1:GFP*, *PIN1:GFP S1,2,3A* or *PIN1:GFP S1,2,3E*, respectively) (Huang et al., 2010) to monitor the effect of phosphorylation on PIN1 vacuolar targeting in different plant tissues. In light-grown seedling roots, the GFP signals were predominantly detected at the PM and almost no intracellular signal was detected in both *PIN1:GFP* and *PIN1:GFP S1,2,3A* mutants (Figures 6A and 6C). To visualize PIN1 vacuolar accumulation in plant tissues, *Arabidopsis* seedlings were shortly incubated in the dark, as it is known to stabilize GFP or GFP fusion proteins in the lytic vacuole (Tamura et al., 2003). Indeed, after 1 hr dark treatment, GFP accumulation in vacuoles was detected in 5-day-old *PIN1:GFP* and *PIN1:GFP S1,2,3A* seedling roots

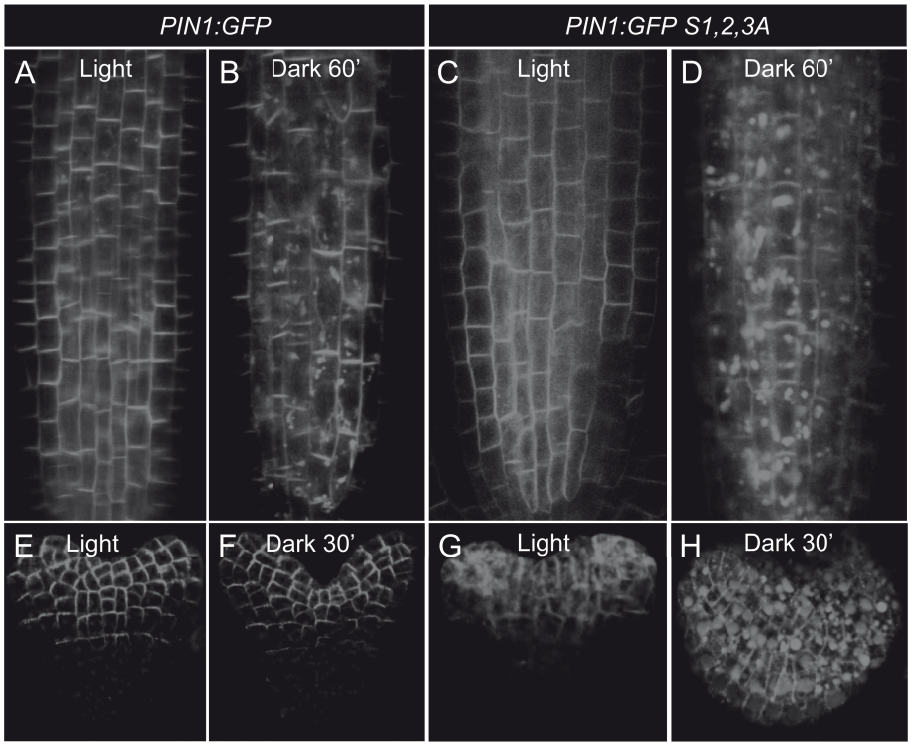

Figure 6. Loss-of-phosphorylation PIN1:GFP shows enhanced vacuolar targeting in *Arabidopsis* embryos and seeding roots.
Dark treatment-induced PIN1 vacuolar targeting in *Arabidopsis* seeding roots (**[A]** to **[D]**) and embryos (**[E]** to **[H]**) is stronger in *PIN1:GFP S1,2,3A* (**[C]**, **[D]** and **[G]**, **[H]**) than in *PIN1:GFP* (**[A]**, **[B]** and **[E]**, **[F]**).

(Figures 6B and 6D). Interestingly, with the same time dark treatment, the vacuolar GFP signal in *PIN1:GFP S1,2,3A* roots (Figure 6D) was stronger than that in *PIN1:GFP* roots (Figure 6B), suggesting that the non-phosphorylatable PIN1:GFP S1,2,3A has an enhanced vacuolar targeting compared to wild type PIN1:GFP.

In the light-grown plants, PIN1:GFP was apically localized in the epidermis of heart-stage embryos (Figure 6E), and PIN1:GFP S1,2,3A was partially PM localized but significantly internalized into endosomes (Figure 6G), consistent with our previous report (Huang et al., 2010). When three-week-old light-grown flowering plants were incubated in dark for 30 minutes, strong vacuolar GFP accumulation could be detected in *PIN1:GFP S1,2,3A* embryos (Figure 6H), but not in *PIN1:GFP* embryos (Figure 6F). Longer dark treatment (2 hrs) also allowed us to observe vacuolar targeting in *PIN1:GFP* embryos (data not shown), indicating that both wild type and loss-of-phosphorylation PIN1:GFP proteins are targeted to the vacuole, but that the rate is higher in the absence

of phosphorylation.

It has been shown that PIN2 vacuolar targeting leads to its degradation (Kleine-Vehn et al., 2008b). To investigate the role of phosphorylation on PIN1 turnover, we incubated light-grown 4-day-old seedlings of the *PIN1:GFP*, *PIN1:GFP S1,2,3A* and

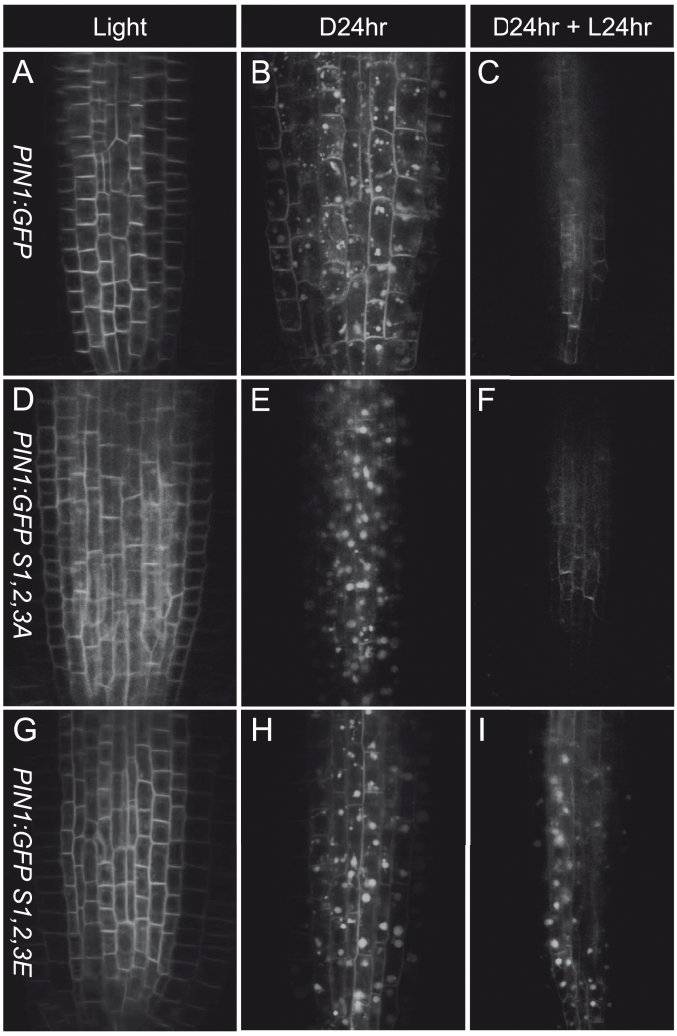

Figure 7. PIN1 vacuolar targeting is irreversible and leads to its degradation.
GFP signals were detected in 4-day-old light-grown seedling roots (**[A]**, **[D]** and **[G]**), or in 3-day-old light-grown seedlings incubated for 24 hrs in the dark (**[B]**, **[E]** and **[H]**), or in 3-day-old light-grown seedlings incubated for 24 hrs in the dark and then transferred back into the light for 24 hrs (**[C]**, **[F]** and **[I]**) of the *PIN1:GFP* line (**[A]** to **[C]**), *PIN1:GFP S1,2,3A* mutant line (**[D]** to **[F]**) and *PIN1:GFP S1,2,3E* mutant line (**[G]** to **[I]**). Incubation in the light did not recover the PIN1:GFP signal at the PM, and instead the GFP signal disappeared, indicating that vacuolar targeting is irreversible and leads to PIN1:GFP degradation.

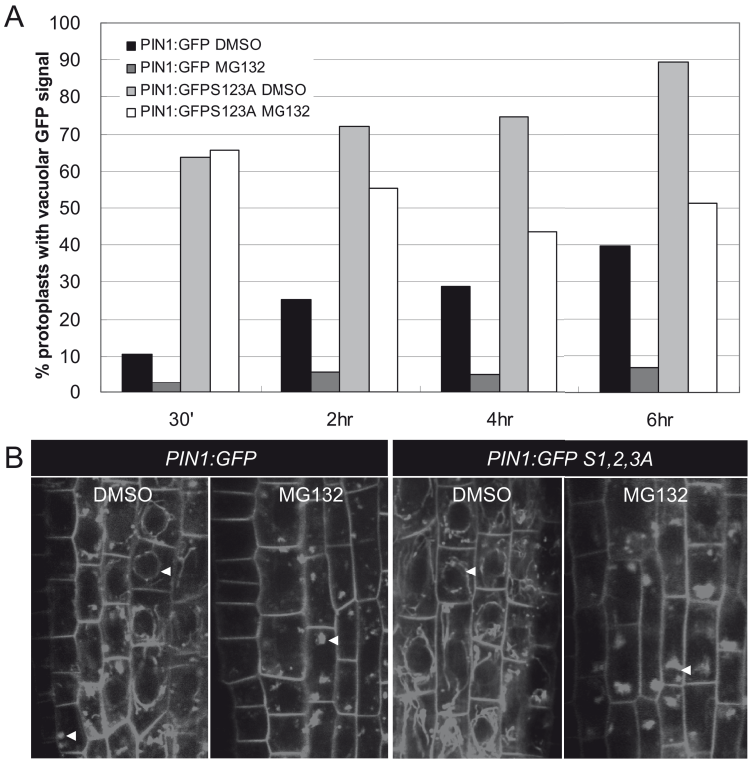

Figure 8. Proteasome activity and PID-mediated phosphorylation affect vacuolar accumulation of PIN1:GFP.
(A) *Arabidopsis* protoplasts were transfected with *PIN1:GFP* (black and dark gray) or *PIN1:GFP S1,2,3A* (light gray and white) and following incubation in darkness for 17 hrs, they were treated with DMSO (black and light gray) or 50 μM MG132 (dark gray and white) for 30 minutes, 2, 4 or 6 hrs.
(B) Seedlings of *Arabidopsis* lines *PIN1:GFP* or *PIN1:GFP S1,2,3A* were grown on solid MA medium in light for 3 days, and then transferred to liquid MA medium containing DMSO or 50 μM MG132 and incubated in the dark for 24 hrs.

PIN1:GFP S1,2,3E lines for 24 hrs in the dark, and then transferred them back to light for 24 hrs. As expected, following dark incubation the vacuolar GFP signal was detected in roots of all seedlings (Figures 7B, 7E and 7H), compared with the PIN1 PM localization in light-grown seedling roots (Figures 7A, 7D and 7G). Strikingly, when seedlings were transferred back to the light, the PIN1:GFP signal at the PM did not recover, and the GFP signal rather disappeared (Figure 7C, 7F and 7I). This indicated that prolonged dark treatment leads to enhanced vacuolar targeting followed by a rapid turnover of PIN1:GFP. Interestingly, the non-phosphorylatable PIN1:GFP S1,2,3A exhibited a more rapid signal loss than wild type PIN1:GFP, whereas turnover of the phosphomimic version PIN1:GFP S1,2,3E was slower.

Previously it was shown that PIN2 turnover and its light-inhibited vacuolar targeting

require the activity of the 26S proteasome, as both processes can be inhibited by incubation with the proteasome inhibitor MG132 (Abas et al., 2006; Laxmi et al., 2008). In our protoplast system, MG132 treatment greatly reduced vacuolar GFP accumulation for both *PIN1:GFP* and *PIN1:GFP S1,2,3A* transfections, although the inhibition effects are different (Figure 8A). Similarly, when 3-day-old light-grown seedlings were incubated for 24 hrs in the dark in medium containing MG132, the vacuolar membrane accumulation in the DMSO treated seedlings (Figure 8B) was inhibited for both wild type and non-phosphorylatable PIN1:GFP proteins. These results confirmed the involvement of proteasome pathway in the PIN vacuolar targeting, and suggested that PID-mediated PIN1 phosphorylation and the proteasome pathway might independently affect targeting of PIN1 to the vacuole.

Model for PID as positive regulator of PAT

The role of PID-phosphorylation as PIN polarity determinant has been well investigated both at the cellular and biochemical levels (Friml et al., 2004; Michniewicz et al., 2007; Kleine-Vehn et al., 2009; Huang et al., 2010). In contrast, the previously proposed role of PID as positive regulator of PAT (Benjamins et al., 2001; Lee and Cho, 2006) has not been extensively studied. Here we used tobacco BY-2 cells, *Arabidopsis* protoplasts and transgenic *Arabidopsis* plant lines expressing wild type or loss- and gain-of-phosphorylation PIN1:GFP proteins to investigate this aspect of PID action in more detail. The tobacco BY-2 cell experiments provided direct evidence that PID activity enhances auxin efflux, implying that PID promotes PIN abundance at the PM. In line with this finding, loss-of-phosphorylation PIN1 and PIN2 showed reduced PM localization and strong internalized signals in embryo and root cells (Chapters 2 and 3). The experiments in *Arabidopsis* protoplasts allowed us to follow the progression of PIN1 subcellular trafficking in time. Early after transfection, newly synthesized PIN1:GFP protein was predominantly found at the PM, and then gradually it became targeted to the vacuole for turnover. The vacuolar accumulation could be easily observed because transfected protoplasts were standardly incubated in the dark, which induces PIN vacuolar accumulation in many plant tissues. Transfering of the protoplasts to the light significantly reduced the vacuolar GFP signal, and PID-mediated phosphorylation also significantly reduced PIN1 vacuolar accumulation, and so maintained PIN1 PM localization. The maintenance of protein PM localization can be attributed to either reduced endocytosis or enhanced exocytosis. However, the detailed mechanisms underlying phosphorylation involvement in specific trafficking pathway are still unclear.

Our data, together with previous reports, lead to a model that explains the dual role

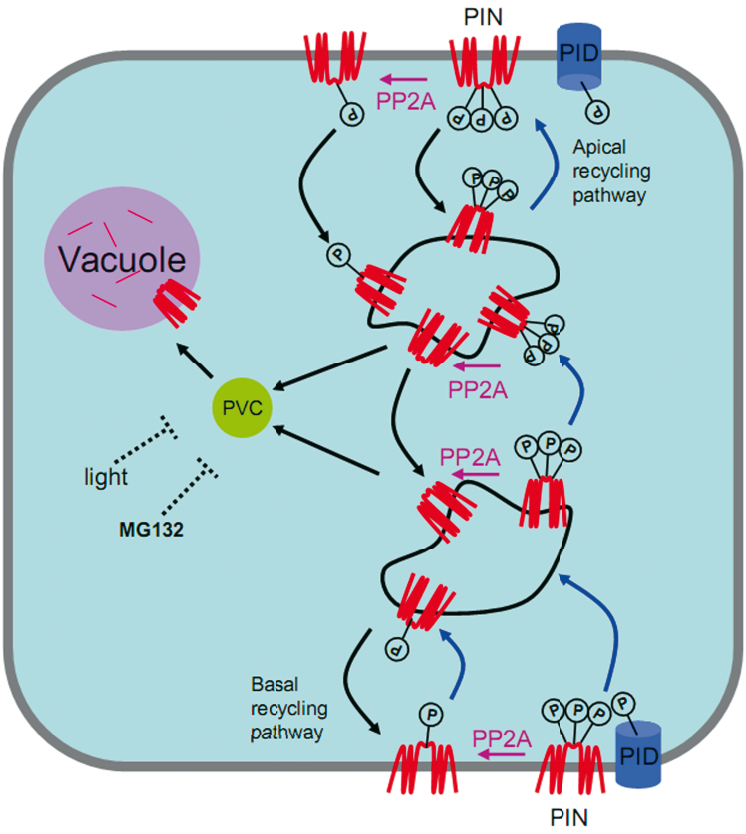

Figure 9. Model describing the dual role of PID as polarity determinant and enhancer of auxin efflux

De novo synthesized PIN proteins arrive at the PM in a non-polar fashion. PIN phosphorylation at three TPRXS(N/S) motifs by the PM-associated PID kinase, directs PIN targeting from the basal to the apical recycling pathway, finally reaching the apical PM. PINs that are only partially phosphorylated, due to the action of the PP2A phosphatases, are recruited back to the basal recycling pathway. As a basal level of phosphorylation is needed for PIN efficient exocytosis and PM localization, non-phosphorylated PINs remain internalized, and are “sitting ducks” for targeting to the vacuole for degradation via the PVC. Light signaling reduces PIN vacuolar targeting, and the proteasome function is also involved as MG132 also inhibits PIN vacuolar targeting.

of PID as PIN polarity determinant on one hand, and enhancer of auxin efflux on the other hand (Figure 9). The function of PID starts when de novo synthesized PIN proteins arrive at the PM in a non-polar fashion (Dhonukshe et al., 2008). Phosphorylation of PINs at all three TPRSX(N/S) motifs by the PM-associated PID kinase, for example the phosphomimic mutation, triggers their recruitment into the apical recycling pathway (chapter 2 and Kleine-Vehn et al., 2009). However when their phosphorylation status is reduced, for example by the PP2A phosphatases action (Michniewitz et al., 2007), they

may be recruited into the basal recycling pathway, where low level phosphorylation is required for PIN efficient exocytosis. When PINs are fully dephosphorylated, they could traffic more easily to the vacuole via PVC (Kleine-Vehn et al., 2008b; Laxmi et al., 2008; Shirakawa et al., 2009). This latter step likely requires a light-regulated downstream event that involves 26S proteasome activity, as this process could be inhibited by light and the proteasome inhibitor MG132. Light probably interferes with this process at the transcriptional level (Laxmi et al., 2008). It is known that proteasome activity is required for the targeting of ubiquitinated membrane proteins to the lysosome or vacuole (van et al., 2001), and PIN2 ubiquitination has been shown to be implicated in its vacuolar targeting (Abas et al., 2006). It will be interesting next to test whether PIN1 is also ubiquitinated and whether the phosphorylation status of PINs affects their ubiquitination, or vice versa.

Materials and methods

Protoplast isolation and transformation

Arabidopsis thaliana Col-0 cell suspension cultures were used for protoplast preparations. Culture maintenance, protoplast isolation and transfections were performed as previously described (Schirawski et al., 2000) with minor modifications. Four-to-six days old cultures were diluted 5-fold in auxin-free Cell Medium (30 g/L sucrose, 3.2 g/L Gamborg's B5 basal medium with mineral organics, adjusted to pH 5.8 with KOH and sterilized by autoclaving), incubated overnight and used for protoplast isolation using auxin-free media. Following transfection, protoplast cells were incubated at 25ºC in the dark for 16-18 hrs before observation or additional treatments.

DNA constructs and mutagenesis

The pBluescript-*35S::PIN1:GFP* vector used for protoplast transformation was described before (Dhonukshe et al., 2007), and *pART7-35S::PID:mRFP* was constructed using the Gateway Technology (Invitrogen). The PID coding region was cloned into pDONOR207 by BP recombination, and subsequently introduced via LR recombination into a Gateway compatible pART7 destination plasmid containing the *CaMV 35S* promoter and the gateway recombinant cassette in frame with the *mRFP* fluorescent marker gene (Galván Ampudia, 2009).

The Quickchange XL site-directed mutagenesis kit (Stratagene) was used to generate mutant constructs. Oligos used for mutagenesis have been described in Table 2 of Chapter 2.

Plant materials and growth conditions

For all experiments, *Arabidopsis thaliana* ecotype Columbia 0 was used. *Arabidopsis* lines *PIN1:GFP*, *PIN1:GFP S1,2,3A* and *PIN1:GFP S1,2,3E* have been described previously (Benková et al., 2003; Huang et al., 2010). Seedlings were grown on MA medium (Masson and Paszkowski, 1992) at 21ºC and a 16 hrs photoperiod. Plants were grown on a mixture of 9:1 substrate soil and sand (Holland Potgrond) at 21ºC, a 16 hrs photoperiod and 70% relative humidity. Transgenic tobacco BY-2 cell lines were obtained by *Agrobacterium*-mediated transformation (Petrásek et al., 2003) using the previously described constructs *pINTAM>>PID* (Friml et al., 2004) and *PIN1::PIN1:GFP* (Benková et al., 2003) have been described before.

Confocal microscopy

Fluorescent signals in *Arabidopsis* roots were observed using a 20x objective of a ZEISS Axioplan microscope equipped with a confocal laser scanning unit. GFP fluorescence was monitored with a 488 nm excitation and a 505-530 nm emission filter. For the protoplast experiments, a Leica DM IRBE confocal laser scanning microscope was used with a 63x water objective. GFP fluorescence was visualized with an Argon laser for excitation at 488 nm and with a 505-530 nm emission filter. The mRFP signal was detected using a laser with a 543 nm excitation and a 560 nm emission filter. A transmitted light image was taken as a reference. Images were processed in ImageJ and assembled in Adobe Photoshop CS2.

Acknowledgements

We thank J. Friml for providing construct *35S::PIN1:GFP*, and C.S. Galván Ampudia for constructing plasmid *35S::PID:mRFP*. We thank G. Lamers for technical help with confocal laser scanning microscopy. This work was supported by grants from the China Scholarship Council (F.H.), and from the Research Council for Chemical Sciences (F.H., CW 700.58.301 to R.O.) with financial aid from The Netherlands Organisation for Scientific Research (NWO).